# In-Situ SAXS Study on the Alignment of Ordered Systems of Comb-Shaped Supramolecules: A Shear-Induced Cylinder-to-Cylinder Transition

**Evgeny Polushkin,*,† Sasa Bondzic,† Joost de Wit,† Gert Alberda van Ekenstein,† Igor Dolbnya,‡ Wim Bras,‡ Olli Ikkala,§ and Gerrit ten Brinke†**

*Laboratory of Polymer Chemistry, Materials Science Centre, University of Groningen, Nijenborgh 4, 9747 AG Groningen, The Netherlands; Dubble CRG/ESRF, Netherlands Organization for Scientific Research (NWO), c/o ESRF, BP 220, F-38043 Grenoble CEDEX, France; and Department of Engineering Physics and Mathematics, Center for New Materials, Helsinki University of Technology, P.O. Box 2200, FIN-02015 HUT, Espoo, Finland*

*Received August 17, 2004; Revised Manuscript Received December 14, 2004*

ABSTRACT: A tooth rheometer, designed to investigate in-situ the influence of large-amplitude oscillatory shear on the macroscopic orientation of complex fluids, is used to study the alignment of two supramolecular systems composed of a polyisoprene-*block*-poly(2-vinylpyridine) block copolymer with octyl gallate (OG) hydrogen bonded to the vinylpyridine block. The molecular ratio $x$ between OG and pyridine groups in these two PI-*b*-P2VP(OG)$_x$ systems is 0.50 and 0.75, respectively. In both cases, a hexagonally ordered cylindrical self-assembly was revealed by small-angle X-ray scattering in a broad temperature range. The spacing of the hexagonal structure decreases significantly on heating and reversibly increases on cooling. In in-situ SAXS experiments, performed with the tooth rheometer, a gradual *macroscopic* alignment of the *nanoscale* structure is observed on heating for both supramolecular systems. The most striking feature is a shear-induced transition from one hexagonal structure to another, more aligned, hexagonal structure observed for PI-*b*-P2VP(OG)$_{0.75}$ in the temperature range 120−140 °C. The transition is accompanied by an abrupt reduction of the domain spacing and additionally by a decrease of the phase angle measured by the rheometer. In the PI-*b*-P2VP(OG)$_{0.5}$ system a comparable reduction in the spacing is observed at 90−95 °C. In this case, it coincides with the most intensive macroscopic alignment of the sample, proceeding in a continuous rather than discontinuous fashion. This behavior is discussed in terms of the breaking of the hydrogen bonds between OG and P2VP being facilitated by shear.

## Introduction

Many research groups are currently involved in the study of self-assembled, mesoscopic materials.[1−19] A very special class of systems consists of so-called comb-shaped supramolecules. These are formed using non-covalent physical interactions, e.g., hydrogen bonding,[4,13,16] ionic bonding,[7,12] or metal coordination,[20,21] to attach side groups to polymeric species. In the case of a diblock copolymer where amphiphilic molecules are physically attached to one of the copolymer blocks, such supramolecules exhibit under certain conditions a self-assembly at two length scales: a large length scale due to the microphase separation between the two blocks and in addition a short length scale ordering inside the comb−block domains.[4,13] A number of peculiar two-length-scale ordered structures have been observed, for example, lamellar-*within*-lamellar and lamellar-*within*-cylinder.[22,23] When the amphiphilic compound acts simply as a filling agent, the nature and spacing of the large length scale self-assembled structure can be readily tailored by varying the amount of amphiphiles.[24] Normally, the self-assembly in block copolymer-based systems gives rise to the formation of a macroscopically isotropic multidomain morphology. For many practical applications, such as membranes, the self-assembled systems should be aligned using a suitable external field. Many options exist as reviewed in ref 9. Two most recent examples, exploiting the role of additional low molar mass species, are discussed in refs 25 and 26. The best known procedure, which is also the subject of the present investigation, consists of imposing a large-amplitude oscillatory shear (LAOS).[3,27−38] The degree of macroscopic alignment can be estimated using electron microscopy and small-angle X-ray (SAXS) and neutron (SANS) scattering techniques. An advantage of SAXS and SANS is the possibility to perform measurements during the shear-induced alignment, and therefore, the data obtained in such in-situ experiments are particularly valuable.

In this paper we report on the alignment of two diblock copolymer-based supramolecules systems composed of a polyisoprene-*block*-poly(2-vinylpyridine) diblock copolymer and octyl gallate molecules hydrogen bonded to the vinylpyridine block. The PI-*b*-P2VP(OG) systems used in this work are considered as good candidates for making nanoscale membranes,[24] and therefore, the examination of their macroscopic alignment under shear is of great importance. It will be shown that the hexagonally ordered cylindrical structure of these systems can be very well aligned macroscopically. However, the two systems investigated, which are very similar in composition, require quite different temperature windows to be well aligned. One of the most interesting findings of this work is the occurrence of a shear-induced cylindrical-to-cylindrical transition for the PI-*b*-P2VP(OG)$_{0.75}$ system in the temperature range 120−140 °C. The simultaneous rheological and synchrotron

† University of Groningen.
‡ Netherlands Organization for Scientific Research.
§ Helsinki University of Technology.
* To whom correspondence should be addressed. E-mail: e.polushkin@rug.nl.

10.1021/ma048314k CCC: $30.25 
Published on Web 02/10/2005

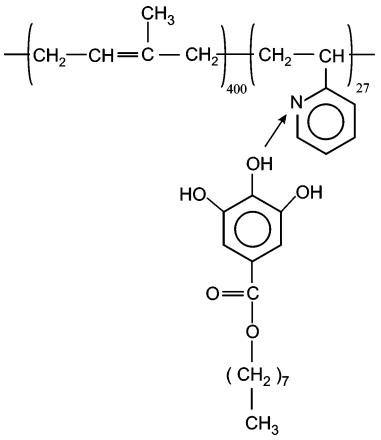


**Figure 1.** Scheme of PI-*b*-P2VP(OG)$_x$ supramolecular complex. Subscript $x$ denotes the ratio between the number of octyl gallate molecules (OG) and pyridine groups of a polyisoprene-*block*-poly(2-vinylpyridine) copolymer (PI-*b*-P2VP).

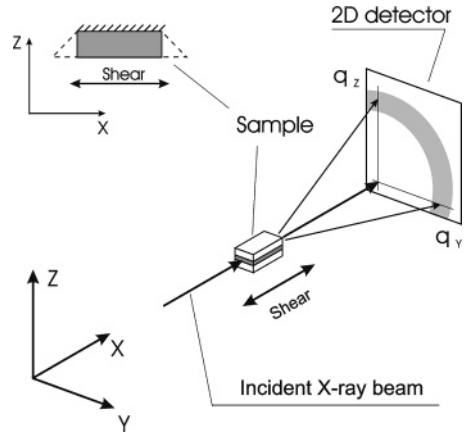


**Figure 2.** Setup used in the in-situ SAXS experiment. A sample is oscillatory sheared in a 0.5 mm gap between two 3 by 5 mm plates (teeth) in the $x-y$ plane. The shear vector and the incident X-ray beam are parallel to the $x$-axis. SAXS patterns are observed in the $y-z$ plane.

SAXS study has been accomplished using a homemade tooth rheometer,[37,38] in which, instead of conventional plate−plate or cone−plate fixtures, two so-called tooth plates are employed. Advantages of this rheometer are the very small amount of sample required, about 30 mg or less, and the possibility to perform in-situ SAXS measurements in two directions.

## Experimental Section

The system under investigation was a complex of poly(1,4-isoprene)-*block*-poly(2-vinylpyridine) and octyl gallate, i.e., 4-octyl-3,4,5-trihydroxybenzoate, attached to the vinylpyridine block due to hydrogen bonds between the hydroxyl groups and the pyridine nitrogen (Figure 1). The diblock copolymer PI-*b*-P2VP with molar masses of 30 and 2.8 kg/mol for the PI and P2VP blocks, respectively, was purchased from Polymer Source, Inc., and used as received. The octyl gallate (OG) obtained from Sigma-Aldrich, Inc., was recrystallized from 9:1 volume ratio mixture of ethanol and chloroform prior to use. Two different PI-*b*-P2VP(OG)$_x$ complexes, with $x = 0.50$ and 0.75 denoting the ratio between the number of OG molecules and pyridine groups, have been investigated. Each of these supramolecules systems was prepared in a way similar to the procedure described elsewhere.[21−23] First, the PI-*b*-P2VP copolymer was dissolved in chloroform to a concentration less than 2% (w/w). Then the required amount of OG was added into the solution, and the system was allowed to form the supramolecular complex for 24 h. After slow evaporation of the solvent in air, the samples were additionally dried in a vacuum at 40 °C for 48 h. Note, the glass transition temperature ($T_g$) of pure P2VP is about 100 °C, while the $T_g$ of the P2VP(OG) domains of the self-assembled PI-*b*-P2VP(OG)$_{0.75}$ is only 33 °C.

SAXS measurements have been performed at the DUBBLE beamline of ESRF in Grenoble, France.[39,40] The sample−detector distance was ca. 8 m, and the X-ray wavelength was $\lambda = 1.24$ Å ($E = 10$ keV). Values of the scattering vector have been calculated as $q = 4\pi/\lambda \sin\theta$, where $\theta$ is one-half a scattering angle. Using a Linkam hot stage, the macroscopically isotropic samples were preliminary examined by SAXS during a heating−cooling run performed with a rate of 10 °C/min. The measuring time in these experiments was 30 s per frame.

Shear-induced alignment of the samples was conducted using a homemade tooth rheometer.[37,38] This rheometer is a modified Bohlin VOR rheometer, specially designed to perform in-situ SAXS studies on the alignment of complex fluids induced by LAOS. The instrument is a kind of plate−plate rheometer, but instead of normally used relatively large plates characterized by a small gap/width ratio, the plates are rather small and look like "teeth". In this study a tooth couple of 5 by 3 mm$^2$ in size has been employed. Despite such a small-size geometry, using the rheometer gives rise to adequate rheological measurements.[38] Its main advantages are (i) the possibility to perform in-situ SAXS measurements in two, *tangential* and *radial*, directions and (ii) the requirement of a very small amount of sample, 30 mg or even less.

In the SAXS experiments carried out in-situ, the measuring time was 60 s per frame. During these measurements performed on heating with a rate not higher than 6 °C/min, the samples have been sheared inside a 0.5 mm gap between the rheometer teeth. The primary X-ray beam of ca. 0.2 by 0.2 mm$^2$ in size was directed into the rheometer gap along the shear vector direction ($x$-axis). Thus, the beam passed through a 5 mm long sample, the thickness of the sample in the shear gradient direction ($y$-axis) was ca. 0.5 mm, determined by the gap, and in the vorticity direction ($z$-axis) the width of the sample was 3 mm (Figure 2). All in-situ SAXS images were obtained as *tangential* patterns in the $q_y-q_z$ scattering plane. The rheometer was operated in a continuous oscillatory mode with a shear strain amplitude of ca. 100% and frequency of 0.7 Hz. On heating the gap between the teeth slightly decreased resulting in an increase (within 20%) in the shear strain. The position of a 2D detector was chosen in such a way that only one quadrant of the scattering pattern could be seen. This allowed us to follow the development of the sample morphology in the $q$ range as broad as 0.06−0.90 nm$^{-1}$. Rheological characteristics, such as the storage and loss moduli $G'$ and $G''$, respectively, as well as the phase angle $\varphi$, were also measured during the in-situ experiments. Note, the oscillatory shear with a 100% strain strongly suggests that the rheological measurements are performed in a nonlinear deformation mode; therefore, the measured characteristics are not truly $G'$ and $G''$, and they should be considered as convenient quantities to follow the alignment of the samples.

## Results and Discussion

**SAXS Measurements on Unsheared Samples.** Since the samples investigated in the preliminary SAXS measurements were macroscopically isotropic, they revealed ringlike images typical for multidomain morphologies. Figure 3 shows the azimuthally averaged SAXS patterns for the PI-*b*-P2VP(OG)$_{0.75}$ system measured in a heating−cooling run with a rate of 10 °C/min performed using a Linkam hot stage. The 1D scattering data have been obtained from the 2D images by integrating the total number of counts at a given distance from the detector spot corresponding to the primary X-ray beam incidence. To provide a more thorough discussion, characteristic SAXS patterns at specific temperatures are shown in Figure 4. At 63 °C,

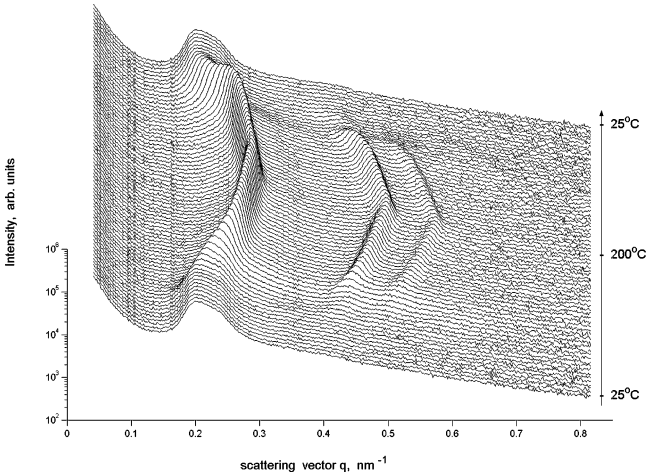


**Figure 3.** 1D SAXS patterns obtained from the nonsheared sample of PI-*b*-P2VP(OG)$_{0.75}$ during a heating−cooling run from 25 to 200 °C and back with a rate of 10 °C/min. For clarity, the curves are uniformly shifted upward.

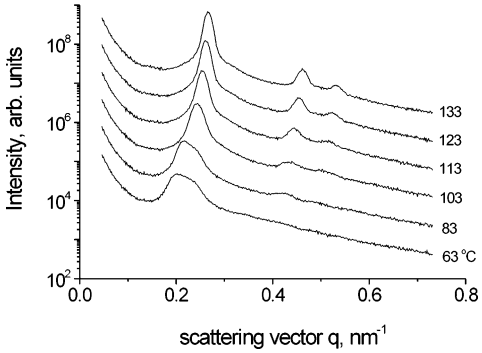


**Figure 4.** Characteristic 1D SAXS patterns taken from Figure 3. On heating to 100 °C the nonsheared sample of PI-*b*-P2VP(OG)$_{0.75}$ reveals a coexistence of LAM and HEX phases, while only the HEX phase is observed at higher temperatures. For clarity, the curves are uniformly shifted upward.

the nonsheared sample reveals mostly a broad peak with the intensity maximum at $q = 0.208$ nm$^{-1}$ and a shoulder at ca. $q = 0.23$ nm$^{-1}$. Additionally, a weak scattering at about $q = 0.4$ nm$^{-1}$ is present, which is hardly visible in Figure 4. We attribute this pattern to the coexistence of lamellar (LAM) and hexagonally ordered (HEX) phases, whose characteristic $d$ spacings are determined by the peak maximum and the shoulder, respectively. The formation of more complex structures, like gyroid or hexagonally perforated lamellar,[41,42] does not seem to take place in this particular supramolecules system. At least, annealing the specimen at 70 °C, which is more than 35 °C above the $T_g$ of the P4VP(OG)$_{0.75}$ domains, for 20 h did not result in any significant modification of the SAXS pattern toward characteristic images of such complex structures. As shown in Figure 4, on heating from 63 to 83 °C the main scattering peak somewhat shifts to higher $q$ values, and two very faint peaks become visible at ca. $q = 0.42$ and 0.50 nm$^{-1}$. Observed together with the double main peak, the new peaks provide additional evidence of the LAM−HEX coexistence, since on further heating they transform into the $\sqrt{3}$ and $\sqrt{4}$ peaks of the HEX phase. The disappearance of the LAM phase is observed at ca. 93 °C as an abrupt shift of the main scattering peak to a higher $q$ value, while its shape becomes Gaussian-like. The SAXS pattern obtained at 103 °C shows three peaks spaced at ratios 1:1.77:2.10, with the first one at $q = 0.244$ nm$^{-1}$. The ratio found at 113 °C is quite close to the characteristic $1:\sqrt{3}:\sqrt{4}$ ratio of a HEX structure, and it remains like that at higher temperatures. Therefore, the SAXS patterns obtained at a relatively fast heating rate of 10 °C/min show that just above 100 °C a single HEX phase becomes thermodynamically favorable. The spacing of the hexagonal structure noticeably decreases on heating and, with a slight difference in temperature, reversibly increases on cooling (Figure 3).

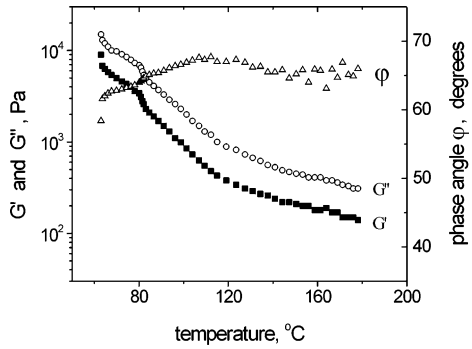


**Figure 5.** Temperature dependences of the dynamic moduli $G'$ and $G''$ and the phase angle $\varphi$ obtained during the shear-induced alignment of PI-*b*-P2VP(OG)$_{0.50}$.

In contrast to PI-*b*-P2VP(OG)$_{0.75}$, SAXS measurements of the PI-*b*-P2VP(OG)$_{0.50}$ system reveal a HEX phase in the whole temperature range investigated, from room temperature up to 200 °C. This sample also shows a considerable decrease of the domain spacing on heating and quite a reversible increase of the spacing on cooling.

Although such a change in $d$ spacing with temperature is a well-known phenomenon for block copolymers, for the systems investigated in this study it is amplified by the H-bonding nature of the complexes. Recently the strong influence of temperature on the H-bonding was demonstrated by IR spectroscopy,[24] and those data were discussed in terms of a reduction in the number of hydrogen bonds between P2VP and OG on heating, resulting in gradual disappearance of the comblike architecture within P2VP(OG) domains. The latter is accompanied by a transformation from initially strongly stretched P2VP chains into more coillike conformations, leading to a decrease in the domain spacing. Such a scenario has also been predicted theoretically.[43]

As noted above, the 2D SAXS images of the quiescent samples were isotropic with respect to the primary X-ray beam, indicating a randomly oriented multidomain morphology. The aim of the shear experiments, to which we will turn our attention next, is to study the influence of shear on the morphology of the PI-*b*-P2VP(OG) systems and, in particular, on their macroscopic alignment, as manifested by the appearance of *anisotropic* SAXS patterns.

**Rheological and in-Situ SAXS Measurements of PI-*b*-P2VP(OG)$_{0.50}$.** Using the tooth rheometer, a sample of the $x = 0.50$ system was subjected to large-amplitude oscillatory shear with a strain amplitude of 100 % and a frequency of 0.7 Hz. Changes of the storage $G'$ and loss $G''$ moduli and the phase angle $\varphi$ measured in the LAOS mode are shown in Figure 5. Characteristic SAXS images obtained for PI-*b*-P2VP(OG)$_{0.50}$ under shear are presented in Figure 6. As seen from Figure 6a, just after loading into the rheometer at ca. 60 °C, the sample shows a slightly anisotropic SAXS pattern. Apart from the first ringlike reflection, showing a maximal intensity

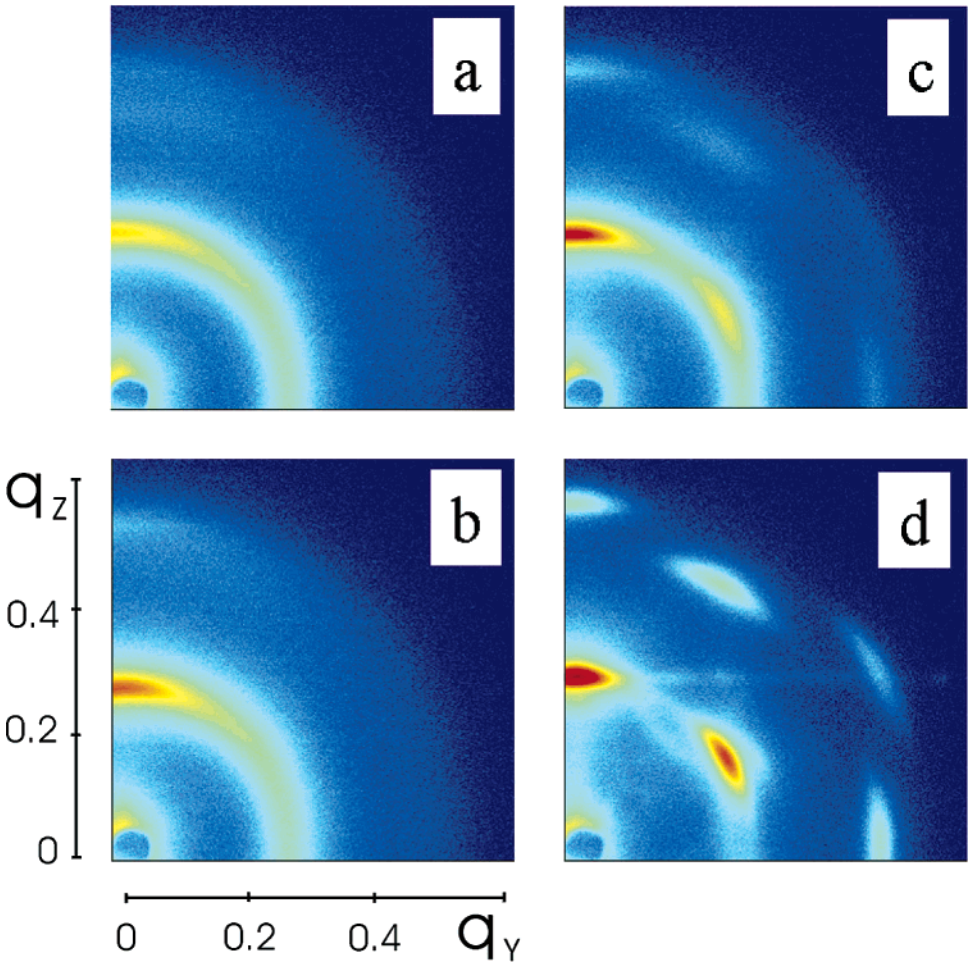


**Figure 6.** Characteristic in-situ SAXS patterns obtained for the PI-*b*-P2VP(OG)$_{0.50}$ sample subjected to the LAOS: (a) at 61 °C just before shear, (b) at 63 °C just after the shear started, (c) at 81 °C, and (d) at 96 °C. The last pattern indicates a nearly perfect *macroscopic* alignment of the HEX *nanoscale* phase (some noisy scattering comes from the polyimide windows of the oven used).

on the meridian at $q = 0.263$ nm$^{-1}$, two more rather faint meridional reflections are observed at ca. $q = 0.46$ and 0.52 nm$^{-1}$. These reflections are spaced at ratios close to $1{:}\sqrt{3}{:}\sqrt{4}$, indicating a HEX structure. It is evident, however, that in general the structure is not aligned yet. When the shear starts, the intensity of the first reflection considerably increases (Figure 6b, 63 °C). At the same time, a significant decrease of the dynamic moduli $G'$ and $G''$ as well as an increase of the phase angle $\varphi$ is detected (Figure 5). As the temperature approaches 80 °C, the sample shows an initial alignment accompanied by further, but more gradual, changes in the rheological parameters and the appearance of additional, rather faint off-meridional reflections in the SAXS images. At 80 °C another quite noticeable decrease of $G'$ and $G''$ and a small increase of $\varphi$ were observed (Figure 5). Just after this, the sample shows a significant improvement in the alignment: an additional off-meridional arc on the first order ringlike reflection and a number of weak higher order reflections located in a position typical for the parallel alignment of a HEX phase[33] are observed at 81 °C (Figure 6c). Gradually developing on heating, the best alignment is observed at temperatures of 95−100 °C. The image obtained at 96 °C is shown in Figure 6d. (Some noisy scattering observed in the pattern comes from the polyimide window of the rheometer oven.) Note, this alignment is *macroscopic*, since the sample illuminated by the primary X-ray beam was 5mm long. Above 140 °C, more and more ringlike scattering patterns of the HEX structure were observed, indicating its partial misalignment. This is probably due to the fact that, as indicated by the high-temperature rheology, the sample is in a very fluid state, where inertia and secondary flow effects can take place.[44]

Interestingly, the changes in the rheological parameters observed at ca. 80 °C and followed by the considerable improvement in the sample alignment coincide with the onset of a significant decrease of the HEX spacing. Figure 7 clearly demonstrates that this decrease is much stronger under shear than in the absence of shear. While below 80 °C the first-order peak is at the $q = 0.26$ nm$^{-1}$ for both the sheared and nonsheared samples, a striking difference is found at higher temperatures where the sheared sample shows lower peak $q$ values. As a result, in the temperature range 85−100 °C, the spacing of the sheared sample decreases by 1.6 nm, from 24.1 to 22.4 nm, while for the nonsheared sample the decrease is 0.4 nm only. The difference in the first order peak position practically vanishes again around 200 °C.

As mentioned above, the strong decrease in domain spacing observed in self-assembled PI-*b*-P2VP(OG) systems on heating is mostly due to the breaking of the hydrogen bonds between octyl gallate and the vinylpyridine block.[24] The results of this study suggest that shear facilitates the hydrogen bond breaking. To specify, the shear applied at low temperatures results in shear-

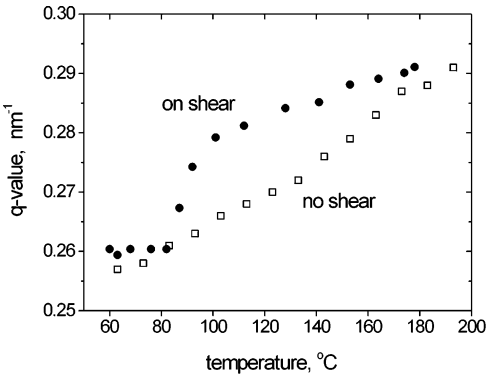


**Figure 7.** Temperature dependences of the position of the main peak observed in the 1D SAXS patterns of the sheared (solid symbols) and nonsheared (open symbols) samples of PI-*b*-P2VP(OG)$_{0.50}$.

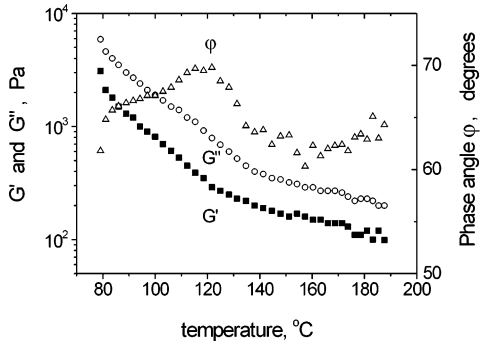


**Figure 8.** Temperature dependences of the dynamic moduli $G'$ and $G''$ and the phase angle $\varphi$ obtained during the shear-induced alignment of PI-*b*-P2VP(OG)$_{0.75}$.

induced changes in the sample morphology. The changes proceed in the course of a slow increase of temperature in time, and they are detected by rheology as a significant decrease of $G'$ and $G''$ and a corresponding increase of $\varphi$ (Figure 5), while SAXS shows that the alignment of the sample remains quite poor (Figure 6). However, above 80 °C the shear stresses applied happen to be high enough to effectively reduce the H-bonding in the comb block, resulting in a drastic decrease in spacing compared to that of the nonsheared sample (Figure 7). This decrease is followed by prominent changes in the rheology and a significant improvement in the macroscopic alignment. Since at high temperatures the number of hydrogen bonds is strongly reduced in both the sheared and nonsheared sample, the SAXS data become again nearly identical (Figure 7).

**Rheological and in-Situ SAXS Measurements of PI-*b*-P2VP(OG)$_{0.75}$.** While eventually a very good alignment was also observed in this case, the shear behavior of the PI-*b*-P2VP(OG)$_{0.75}$ system was quite different from that of PI-*b*-P2VP(OG)$_{0.50}$. A sample of $x = 0.75$ was loaded into the rheometer at ca. 60 °C and then heated to 78 °C without any shear. When at 79 °C the shear starts, a considerable decrease of the dynamic moduli $G'$ and $G''$ and an increase of the phase angle $\varphi$ are observed (Figure 8). On further heating, the rheological measurements show a gradual recession of both $G'$ and $G''$ moduli in a similar manner as reported above for PI-*b*-P2VP(OG)$_{0.50}$ (see Figure 5).

In contrast to the $x = 0.5$ sample, the $x = 0.75$ sample showed a quite peculiar nonmonotonic behavior of the phase angle $\varphi$ with temperature. Figure 9 shows the temperature dependence of $\varphi$ presented together with characteristic SAXS images observed during the in-situ measurements. Like the $x = 0.5$ sample, the $x = 0.75$ sample scattered somewhat anisotropically just after being squeezed between the rheometer teeth. The pattern obtained at 76 °C is a typical image recorded before the shear is started. In contrast to the $x = 0.5$ sample, the first image of the $x = 0.75$ sample obtained under shear at 79 °C appears to be very akin to that obtained at 76 °C. However, a closer look at these two images reveals that the primary arc reflection at ca. $q = 0.22$ nm$^{-1}$ becomes more isotropic at 79 °C if compared to that at 76 °C. This response to shear is quite different from that of a pure lamellar system where three orders of sharp meridional reflections are observed.[37] As will be shown below, it indicates an initial alignment of the HEX domains along the shear direction. Such an alignment is already rather evident at 94 °C when two new off-meridional arcs are observed in positions close to that of the (100) and (110) reflections of a HEX structure. These new reflections are well visible in the image obtained at 100 °C (Figure 9).

Before discussing the data shown in Figure 9 further, it is worthwhile to consider characteristic 1D SAXS patterns of the $x = 0.75$ sample in more detail, since its morphological behavior under shear happened to be quite complex. The pattern obtained at 61 °C reveals three meridional peaks: a relatively narrow one at $q = 0.220$ nm$^{-1}$ and two broad peaks located at $q = 0.415$ and 0.623 nm$^{-1}$ (Figure 10a). The second peak has evidently a shoulder at ca. $q = 0.46$ nm$^{-1}$. The positions of the peaks again strongly suggest that a coexistence of LAM and HEX phases takes place. We suppose that the first-order peak of the LAM phase should be located at $q = 0.208$ nm$^{-1}$ and that the peaks at 0.415 and 0.623 nm$^{-1}$ can be assigned to the second- and third-order reflections. As discussed above, a similar $q$ value, 0.209 nm$^{-1}$, was found for the first peak of the nonsheared sample at 63 °C. Given this assignment, the somewhat different position of the primary peak observed at 0.220 nm$^{-1}$ and the presence of the shoulder at $q = 0.46$ nm$^{-1}$ on the second peak are consistent with the presence of a HEX phase with a first-order peak at about 0.225 nm$^{-1}$. The $\sqrt{3}$, $\sqrt{4}$, and $\sqrt{7}$ peaks of the HEX phase are expected at $q = 0.39$, 0.45, and 0.60 nm$^{-1}$, respectively. In principle, the first two peaks can contribute to the broad peak observed at around 0.415 nm$^{-1}$, while the expected position of the $\sqrt{7}$ peak is too low to appear as the one at 0.623 nm$^{-1}$, assigned above to the third order of the LAM phase. In any case, the presence of the $\sqrt{7}$ peak is unlikely since it requires a quite good ordering of the HEX phase, which is hardly achievable under conditions of two phase coexistence. Thus, the peak at 0.623 nm$^{-1}$ can be considered as an indicator for the presence of the LAM phase.

Despite the 2D images do not reveal many changes on heating to 80 °C, the 1D SAXS pattern obtained at 76 °C is quite different from that at 61 °C (Figure 10a). In the former, the second peak is clearly double, showing a maximum at 0.416 nm$^{-1}$ and a prominent shoulder at 0.465 nm$^{-1}$. The first peak is observed at $q = 0.228$ nm$^{-1}$, and the third one is located at 0.627 nm$^{-1}$. Therefore, in general the scattering pattern still suggests two-phase coexistence. After the shear started at 79 °C, apart from the above-mentioned "isotropization" observed in the 2D image (Figure 9), the corresponding 1D pattern demonstrates a development in the shape of the second and third peak (Figure 10a). The latter

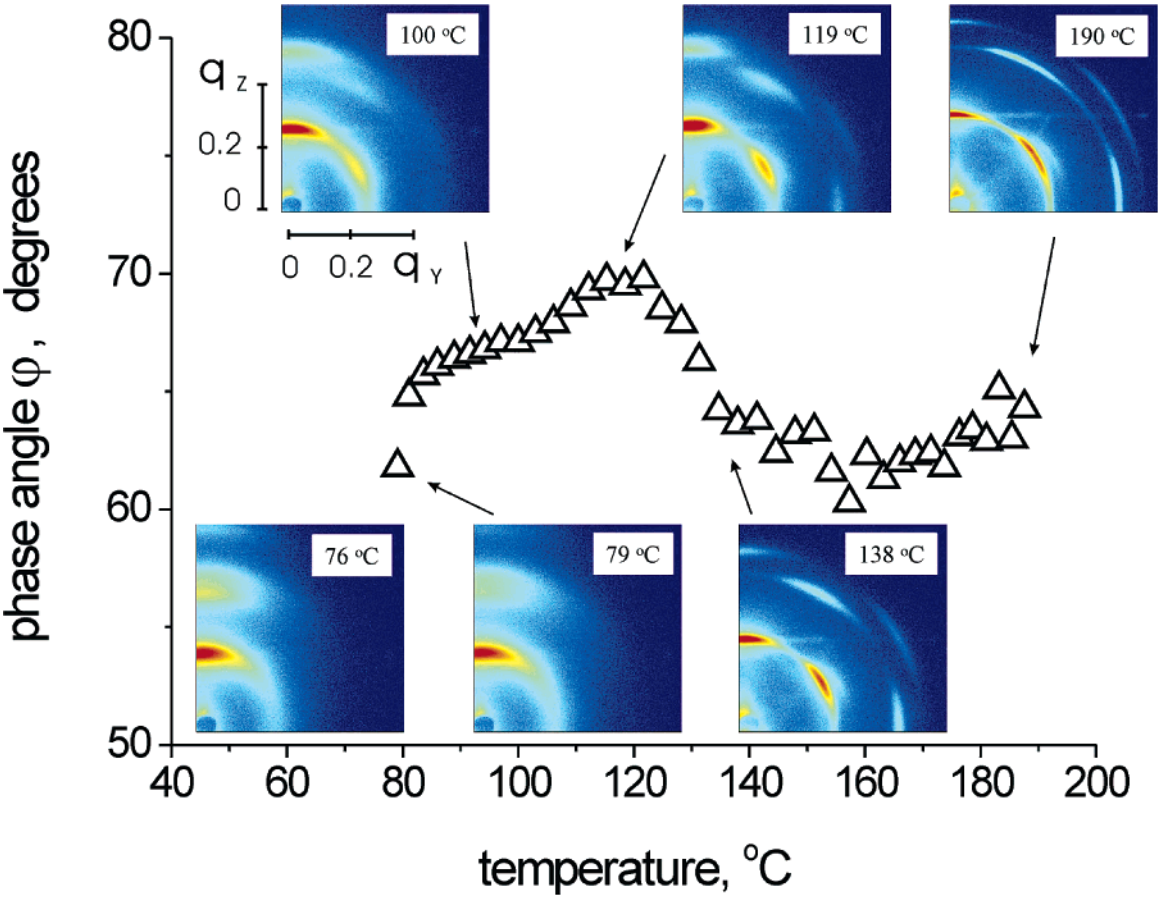


**Figure 9.** Changes of the phase angle $\varphi$ with temperature and characteristic in-situ 2D SAXS patterns recorded during the shear-induced alignment of PS-*b*-P2VP(OG)$_{0.75}$. A very good macroscopic alignment of the 5 mm long sample is observed at temperatures from 120 to 140 °C where $\varphi$ significantly decreases.

becomes broader and weaker compared to that at 76 °C. Since the third peak has been assigned to the LAM phase, this indicates that the LAM phase disappears and transforms into a cylindrical structure. Changes in the shape of the second peak also support this. The intensity of the maximum at 0.419 nm$^{-1}$ decreases, while that of the shoulder at 0.466 nm$^{-1}$ increases. It is well-known that in principle either the second-order or the third-order reflection of a LAM phase can be extinguished due to the form factor. In our case, however, the drop in intensity is observed simultaneously for the two peaks at ca. 0.42 and 0.63 nm$^{-1}$ ascribed to the LAM phase, indicating its transformation to a HEX phase.

It is important to mention that a decrease in the intensity of the peak at 0.42 nm$^{-1}$ observed at 79 °C is not in disagreement with the dominance of the HEX phase, which is expected to give the $\sqrt{3}$ peak at ca. 0.40 nm$^{-1}$, considering the position of the primary peak at this temperature. It is known that cylinders formed during a LAM-to-HEX transition lie in the planes of disappearing lamellae,[45,46] and on shear the (100) plane of a HEX phase is usually parallel to the shear plane.[33] Therefore, after the initial alignment achieved at loading the sample into the rheometer (see the image at 76 °C in Figure 9), the sheared sample is expected to show a prominent $\sqrt{3}$ peak, as well as the $\sqrt{7}$ one, only when HEX domains are well aligned along the shear vector.

As seen from Figure 10a, at 106 °C the sample reveals the HEX phase peaks at $q$ = 0.245, 0.436, and 0.491 nm$^{-1}$, shifting to 0.248, 0.442, and 0.493 nm$^{-1}$ at 113 °C, respectively. Besides, a very weak peak is observed at ca. 0.73 nm$^{-1}$, which is believed to be the $\sqrt{9}$ reflection of the HEX phase.

Returning to Figure 9, one can see that, after an initial strong increase in the phase angle $\varphi$ at low temperatures, it approaches a plateau value of ca. 67° at 100 °C, and then a new increase of $\varphi$ up to 70° is observed on further heating to 120 °C. The latter increase is in good correlation with the beginning of the macroscopic alignment of HEX domains along the shear, which as been mentioned above is already visible in the SAXS image at 94 °C and becomes evident at 100 °C. At 119 °C a series of anisotropic reflections of the HEX phase are clearly observed in the 2D image shown in Figure 9. On further heating, however, a considerable decrease of the phase angle $\varphi$ down to 64° was detected, while the SAXS pattern obtained at 138 °C, showing narrow and uniformly intensive arc reflections, indicates an additional improvement in the sample alignment. Above 150 °C a misalignment of the HEX structure was detected as the gradual appearance of a ringlike background scattering. The SAXS pattern obtained at 190 °C (Figure 9), which is very similar to the corresponding patterns of PI-*b*-P2VP(OG)$_{0.50}$, is a typical image showing the high-temperature misalignment.

It has turned out that the improvement in alignment followed by the decrease of $\varphi$ is accompanied by striking changes in the samples morphology. In fact, above 120 °C a new meridional reflection is observed next to the (200) one at somewhat higher angles (Figure 11). At 125 °C these two reflections are at $q$ = 0.503 and 0.532 nm$^{-1}$, and they shift to 0.508 and 0.541 nm$^{-1}$ at 131 °C, respectively. The changes on the meridian are ac-

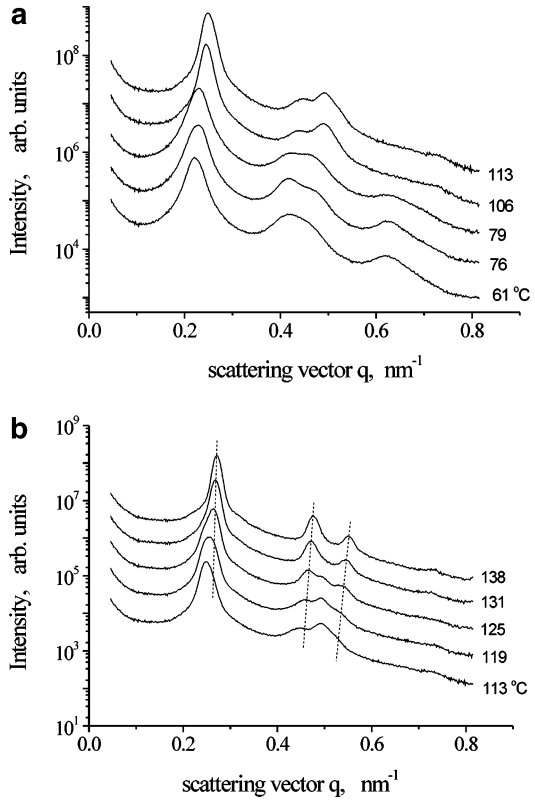


**Figure 10.** Characteristic 1D SAXS patterns obtained upon the alignment of PI-*b*-P2VP(OG)$_{0.75}$. (a) Transformation of the LAM−HEX coexistence to the HEX phase under shear started at 79 °C. (b) Shear-induced transition of the HEX phase H1 to the H2. The dashed lines show the expected positions of the 1, $\sqrt{3}$, and $\sqrt{4}$ peaks of the H2 phase at lower temperatures. For clarity, the curves are uniformly shifted upward.

companied by the appearance of a corresponding prominent arc in the vicinity of the (200) off-meridional reflection, which was rather faint at 119 °C. At 138 °C the new meridional reflection becomes already quite intensive while the neighboring one at a somewhat smaller $q$ value is practically extinguished. Besides, the 2D images demonstrate a similar transformation of the (100) reflections. In the region of 119−125 °C the meridional reflection broadens to higher $q$ values, while the off-meridional one just moves to higher $q$ values. At 131−138 °C the former becomes narrower and shows the intensity maximum at $q$ values similar to that of the off-meridional reflection. As for the (110) reflections, only one of these is well visible at 119 °C as an off-equatorial arc, quite broad in the radial direction. At 125 °C both this arc and another reflection are observed at remarkably higher $q$ values, becoming rather sharp and more intensive.

Additional insight into the morphological changes that occur at elevated temperatures can be obtained from Figure 10b. For better comparison, the curve at 113 °C previously shown in Figure 10a is presented here again. At this temperature the primary peak at $q$ = 0.246 nm$^{-1}$ is noticeably narrower than at 119 and 125 °C, observed at somewhat higher $q$ values. In the latter case, the peak is at 0.262 nm$^{-1}$ and clearly has a shoulder at ca. $q$ = 0.248 nm$^{-1}$. Additionally, a broad triple peak is observed at higher $q$ values at these two temperatures. The patterns obtained at 131 and 138 °C reveal four peaks spaced at ratios of 1:1.75:2.03:2.69, indicating a HEX structure. Dashed lines are drawn through the first three peaks in order to show the expected position of the corresponding peaks at lower temperatures. As seen from the picture, at 113 °C the peaks ascribed above to the HEX structure are not located at the expected positions. All this is strong evidence for a specific shear-induced transition from a HEX structure H1 to another HEX structure H2 occurring in the temperature region of ca. 120−140 °C, where a decrease of the phase angle $\varphi$ was also observed.

Figure 12 shows the temperature dependence of the position, intensity, and half-width at half-maximum (hwhm) of the primary peak observed in the 1D SAXS patterns of the sheared samples. There are two temperature regions, from 70 to 80 °C and from 110 to 135 °C, where the hwhm passes over a maximum while the $q$ value of the peak suddenly increases and its intensity somewhat drops. Such behavior of these parameters clearly indicates the morphological changes discussed above. Interestingly, the data obtained at low temperatures suggest that the coexistent LAM phase starts disappearing and transforming to the HEX phase below 79 °C where the shear started.

Figure 13 gives a general overview of the behavior of the PI-*b*-P2VP(OG)$_{0.75}$ system, comparing the main changes in the SAXS patterns of the sheared and nonsheared samples. Above 140 °C three orders of the HEX phase H2 are observed for the sheared samples (up triangles), and their position is in good agreement with that of the HEX phase observed in the nonsheared samples (open circles). However, there is a clear difference in the position of peaks observed at low temperatures, where the LAM−HEX coexistence was revealed for both samples. For example, at 73 °C the sample measured in the rheometer (solid squares) shows the main peak at $q$ = 0.223 nm$^{-1}$, whereas the value for the nonsheared sample (open squares) is 0.209 nm$^{-1}$ only. In the former case, the main peak and two other peaks are spaced at ratios 1.08:2.00:3.03, indicating that the position of the first-order peak of the LAM phase is strongly affected by the presence of the HEX phase. At 83 °C these three peaks are already spaced at ratios 1.00:1.77:2.01, suggesting that the HEX phase H1 becomes the major phase in the two-phase coexistence, denoted in Figure 13 as L + H1. Above 100 °C the presence of the LAM phase in the sheared sample is unlikely since the peaks are nearly in the ratio of 1:$\sqrt{3}$:$\sqrt{4}$ at 106 and 113 °C (down triangles show the H1 phase). The nonsheared sample at these temperature shows two first peaks at $q$ values that are quite similar those of the sheared sample. An evident discrepancy between the samples is observed at higher $q$ values, where the nonsheared sample gives a very weak and broad peak (see Figure 4), due probably to imperfections in the cylinders order.

The shear-induced transition of the HEX phase from the H1 structure (down triangles) to the H2 structure (up triangles) first appears as a sudden increase in the $q$ value value of the $\sqrt{3}$ peak at 119 °C (Figure 13). Besides, the position of the off-meridional (100) and (200) reflections becomes somewhat different from that on the meridian at this temperature. At 125 and 131 °C the reflections of both the H1 and H2 structures are simultaneously observed, while only the HEX phase H2 is present on further heating. The data shown in Figure 13 indicate that the $d$ spacing is slightly smaller than that observed for the nonsheared sample.

**Morphology and Shear Behavior.** As revealed by SAXS, a very good macroscopic alignment has been

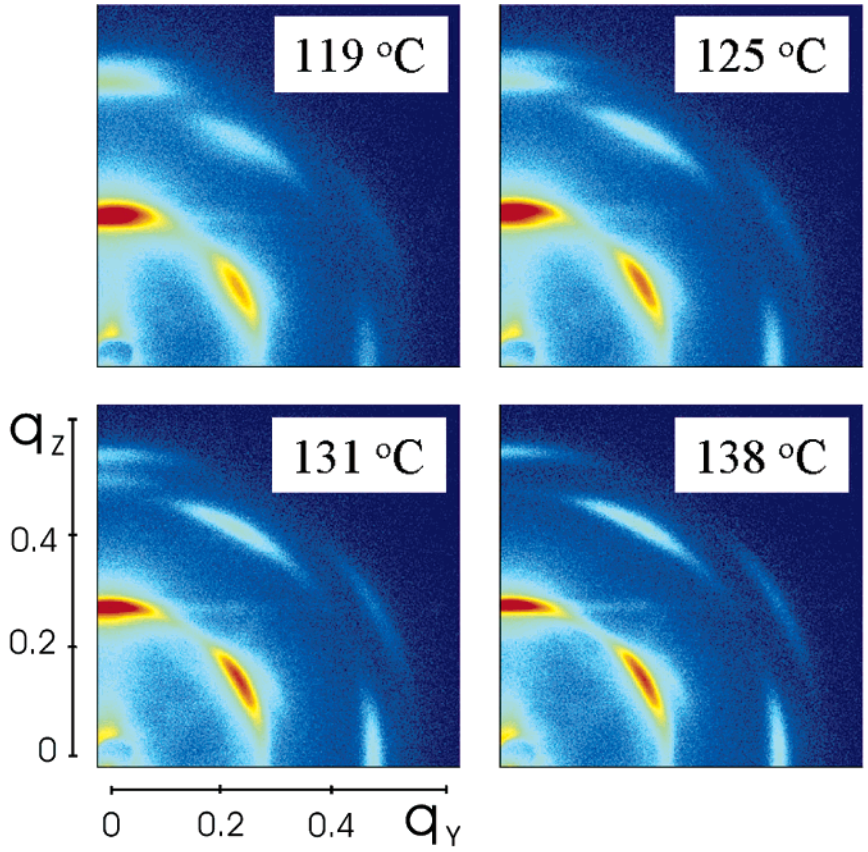


**Figure 11.** In-situ SAXS patterns of the sheared PI-*b*-P2VP(OG)$_{0.75}$ sample at 119−138 °C.

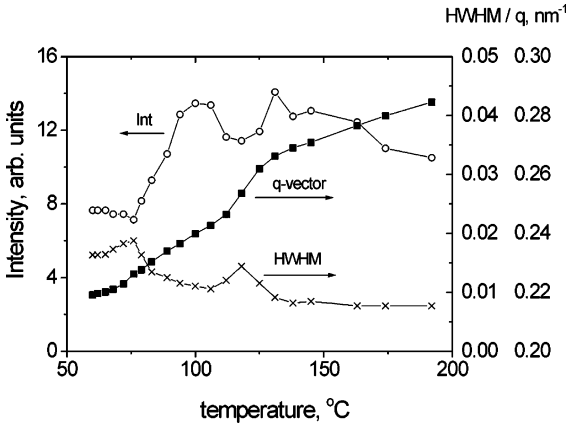


**Figure 12.** Temperature dependences of the intensity, position, and half-width at half-maximum (hwhm) of the main peak observed in the 1D SAXS patterns of the sheared sample of PI-*b*-P2VP(OG)$_{0.75}$.

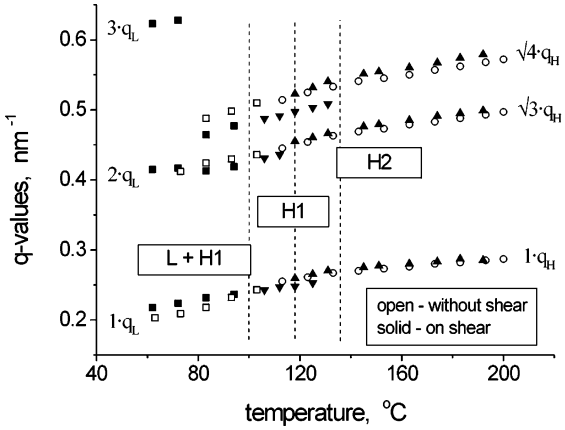


**Figure 13.** Position of the main peaks observed in the 1D SAXS patterns of the sheared (solid symbols) and nonsheared (open symbols) samples of PI-*b*-P2VP(OG)$_{0.75}$ on heating. A coexistence of LAM and HEX phases is revealed at low temperatures (L + H1, squares). Above 120 °C a shear-induced transition from the HEX structure H1 (down triangles) to another structure H2 (up triangles) is observed while the nonsheared sample shows a gradual decrease of the HEX phase spacing on heating (circles).

achieved in both the $x = 0.50$ and $x = 0.75$ supramolecular systems subjected to LAOS. Still, despite using the same shear procedure, i.e., shearing in a 0.5 mm gap with a strain amplitude of 100% and a frequency of 0.7 Hz, the behavior of these two systems and the temperature range, where they showed the most prominent alignment, is quite different. In the case of PI-*b*-P2VP(OG)$_{0.50}$, a clear indication for the sample alignment was revealed below 100 °C, while for PI-*b*-P2VP(OG)$_{0.75}$ this happened in the temperature range from 120 to 140 °C. This difference in temperature conditions and the different morphological behavior of the samples under shear, which were readily observed in the in-situ SAXS experiments, will now be discussed.

PI-*b*-P2VP(OG)$_{0.75}$ differs from PI-*b*-P2VP(OG)$_{0.50}$ by showing LAM−HEX coexistence at low temperatures. Because of this, the coexisting lamellae and cylinders could be easily aligned parallel to the $x-y$ plane (see Figure 2) during the loading procedure at 60 °C. The 2D image obtained at 76 °C gives direct evidence that such an alignment was preferred (Figure 9). We suppose that just above 80 °C, when the shear starts, the flow is not uniform and occurs mostly along the disappearing LAM phase, while the deformation of HEX domains is relatively small. It can be also assumed that inside the

HEX domains the PI phase is mainly affected by the shear while the cylinders formed by the P2VP(OG) blocks are randomly oriented in the $x-y$ plane and flow cooperatively along the (100) planes, forming layers of nonaligned cylinders. The experimental data obtained indicate that the LAM phase tends on shear to transform into the HEX phase. As seen from Figure 12, a noticeable decrease of the hwhm of the primary peak was observed just after applying the shear, indicating the tendency to form a single phase. The presence of the characteristic $\sqrt{3}$ peak in the corresponding 1D SAXS patterns shows that this phase is mostly HEX (see Figures 10a and 13). On the other hand, residues of the LAM phase are expected to remain up to ca. 100 °C. As a result, on heating the PI-*b*-P2VP(OG)$_{0.75}$ sample a relatively good macroscopic alignment of the HEX structure was observed above 120 °C only, while for the PI-*b*-P2VP(OG)$_{0.50}$ system this occurred below 100 °C. Interestingly, at 80−100 °C the values of $G'$, $G''$, and $\varphi$ measured for the $x = 0.75$ system are quite similar to those of the $x = 0.5$ sample (cf. Figures 5 and 8).

In the temperature range 100−120 °C, where the LAM phase is no longer present, the alignment of the PI-*b*-P2VP(OG)$_{0.75}$ occurs under shear stresses that are 4−5 times weaker than those measured during the alignment of PI-*b*-P2VP(OG)$_{0.50}$ at 70−90 °C. Under these conditions, the development of the sample morphology proceeds without a noticeable decrease in the number of hydrogen bonds caused by shear. At about 120 °C the sample is already rather well aligned. Upon further heating the shear stresses slightly decrease but remain apparently high enough to affect the hydrogen bonds, which are considerably weakened with increasing temperature.[24] The consequence of this is a shear-induced H1 to H2 transition of the hexagonal phase, accompanied by further alignment and decrease of the phase angle $\varphi$ as revealed in the rheological measurements.

Figure 14 illustrates the main points of this transition. Because of the strong hydrogen bonding with OG molecules at low temperatures, P2VP chains adopt a rather stretched conformation.[23,43] Because of this, the diameter of the P2VP(OG) cylinders and therefore the spacing of the HEX structure H1 are relatively large. Upon heating the number of H-bonds is gradually decreasing, resulting in a decrease of the cylinder diameter, since P2VP chains, being surrounded by free OG molecules, are now in a more coillike conformation (Figure 14a). An applied shear aligns the HEX structure and at a certain temperature becomes suddenly able to break many several hydrogen bonds between P2VP and OG, giving rise to an abrupt reduction in the diameter of the cylinders (Figure 14b). As a consequence, the PI conformations become equally less stretched, and all this results in the formation of the HEX phase H2. Since the latter is a somewhat more densely packed cylindrical structure than the initial H1 phase, the rheological measurements show the reported decrease in the phase angle $\varphi$, implying a more elastic response. Similar phase angle dependencies have also been observed for the PI-*b*-P2VP(OG)$_{1.00}$ system, the behavior of which examined under various shear conditions will be reported elsewhere.[47] As for the PI-*b*-P2VP(OG)$_{0.50}$ system, after achieving the significant alignment at low temperatures, which was accompanied by an increasing $\varphi$, the comb structure of the system is thought to be already considerably destroyed. After this, only a very small decrease of the phase angle $\varphi$ has been observed on heating from 110 to 140 °C (Figure 5).

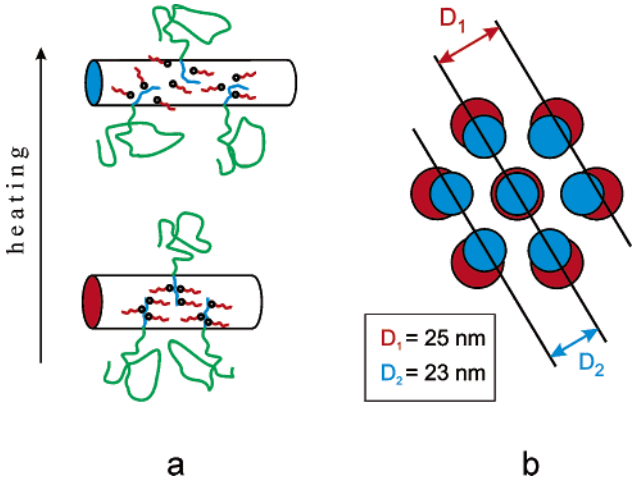


**Figure 14.** Cartoons of the morphological changes in PI-*b*-P2VP(OG)$_{0.75}$ caused by breaking of the hydrogen bonds on heating. (a) At low temperatures the P2VP chains are severely stretched due to the strong bonding with OG molecules, while at elevated temperatures they are surrounded by free OG and adopt a more coillike conformation. (b) Under shear the breaking process is facilitated and at a certain temperature a shear-induced transition from the H1 structure to the more densely packed H2 structure is observed.

## Concluding Remarks

The experiments reported demonstrate that the tooth rheometer used in this work is a very convenient tool to study the behavior of complex supramolecular systems under oscillatory shear by means of in-situ SAXS or other scattering techniques. For both PI-*b*-P2VP(OG)$_{0.50}$ and PI-*b*-P2VP(OG)$_{0.75}$ systems investigated, it has been shown that their nanoscale HEX structure can be very well aligned macroscopically using LAOS. The macroscopic alignment is evidenced by the anisotropic SAXS patterns that were obtained in-situ from the 5 mm long samples being sheared in the rheometer. In each of the two cases, the temperature conditions for optimal alignment are different, and they are mostly determined by the morphology of the systems rather than the duration of the shear applied. For PI-*b*-P2VP(OG)$_{0.50}$ a very good alignment was observed at 90−100 °C while for PI-*b*-P2VP(OG)$_{0.75}$ the corresponding temperature range was from 120 to 140 °C. In the latter system a LAM−HEX coexistence has been observed below 100 °C. The SAXS experiments performed in-situ allowed us to readily display the difference in the shear behavior of the two samples.

It has turned out that the phase angle $\varphi$ was the most sensitive rheological parameter to follow the morphological changes during the alignment. While the dynamic moduli $G'$ and $G''$ show a more or less gradual decrease in values with temperature, the dependences of the phase angle $\varphi$ obtained for both samples happens to be quite nonmonotonic. Apart from the initial increase of $\varphi$ in the early stages of the alignment, a decrease of $\varphi$ has been observed at later stages involving higher temperatures. For example, for the PI-*b*-P2VP(OG)$_{0.75}$ sample, which shows the most prominent decrease, the phase angle drops from 70° to 64° when the temperature increases from 120 to 140 °C. In the same temperature region an abrupt decrease in the spacing of the HEX phase has been observed. Such a behavior of the PI-*b*-

P2VP(OG)$_{0.75}$ sample, as well as somewhat different behavior of PI-*b*-P2VP(OG)$_{0.50}$, is thought to be consistent with our recently reported viewpoint on the nature of morphological changes observed in PI-*b*-P2VP(OG) systems with temperature. The idea is that on heating the number of hydrogen bonds between OG molecules and PVP chains decreases. This leads to a significant reduction in the nanoscale structure spacing due to a gradual change from stretched conformations of PVP chains to more coillike ones.[24,43] In this study it has been argued that under shear the process of hydrogen bond breaking is noticeably facilitated and is manifested as a shear-induced decrease of the domain spacing. In the case of PI-*b*-P2VP(OG)$_{0.75}$, this transition was revealed by rheology and SAXS in the temperature region of 120−140 °C, after the sample had already been rather well aligned. The PI-*b*-P2VP(OG)$_{0.5}$ system showed a more gradual decrease of the spacing at 80−100 °C, accompanied by a considerable alignment of the sample.

Finally, we would like to note that although the experimental data obtained under shear are very consistent with the molecular model suggested, any direct evidence for the shear-induced breaking of hydrogen bonds is not available yet. Additional experiments have already been planned for the near future to verify this hypothesis.

**Acknowledgment.** Beamtime on the DUBBLE beamline of ESRF (Grenoble, France) has kindly been made available by The Netherlands Organization for Scientific Research (NWO). Jeroen Jacobs is acknowledged for the technical support during the in-situ SAXS experiments. This work has been supported as part of the European Science Foundation Collaborative Research (EUROCORES) Programme on Self-Organised NanoStructures (SONS).

## References and Notes

(1) Cochran, E. W.; Bates, F. S. *Phys. Rev. Lett.* **2004**, *93*, 087802.
(2) Davidock, D. A.; Hillmyer, M. A.; Lodge, T. P. *Macromolecules* **2004**, *37*, 397.
(3) Hamley, I. W.; Castelletto, V.; Mykhaylyk, O. O.; Gleeson, A. J. *J. Appl. Crystallogr.* **2004**, *37*, 341.
(4) Ikkala, O.; ten Brinke, G. *Chem. Commun.* **2004**, *19*, 2131.
(5) Hamley, I. W. *Angew. Chem., Int. Ed.* **2003**, *42*, 1692.
(6) Hashimoto, T.; Yamauchi, K.; Yamaguchi, D.; Hasegawa, H. *Macromol. Symp.* **2003**, *201*, 65.
(7) Faul, C. F. J.; Antonietti, M. *Adv. Mater.* **2003**, *15*, 673.
(8) Antonietti, M. *Nat. Mater.* **2003**, *2*, 9.
(9) Park, C.; Yoon, J.; Thomas, E. L. *Polymer* **2003**, *44*, 6725.
(10) Kato, T. *Science* **2002**, *295*, 2414.
(11) Mortensen, K.; Theunissen, E.; Kleppinger, R.; Almdal, K.; Reynaers, H. *Macromolecules* **2002**, *35*, 7773.
(12) Thünemann, A. F. *Prog. Polym. Sci.* **2002**, *27*, 1473.
(13) Ikkala, O.; ten Brinke, G. *Science* **2002**, *295*, 2407.
(14) Krishnan, K.; Almdal, K.; Burghardt, W. R.; Lodge, T. P.; Bates, F. S. *Phys. Rev. Lett.* **2001**, *87*, 098301.
(15) Fasolka, M. J.; Mayes, A. M. *Annu. Rev. Mater. Res.* **2001**, *31*, 323.
(16) Kato, T.; Mizoshita, N.; Kanie, K. *Macromol. Rapid Commun.* **2001**, *22*, 797.
(17) Muthukumar, M.; Ober, C. K.; Thomas, E. L. *Science* **1999**, *277*, 1225.
(18) Hashimoto, T.; Ogawa, T.; Sakamoto, N.; Ichimiya, M.; Kim, J. K.; Han, C. D. *Polymer* **1998**, *39*, 1573.
(19) Whitesides, G. M.; Mathias, J. P.; Seto, C. T. *Science* **1991**, *254*, 1312.
(20) Valkama, S.; Lehtonen, O.; Lappalainen, K.; Kosonen, H.; Castro, P.; Repo, T.; Torkkeli, M.; Serimaa, R.; ten Brinke, G.; Leskelä, M.; Ikkala, O. *Macromol. Rapid Commun.* **2003**, *24*, 556.
(21) Ruokolainen, J.; Tanner, J.; ten Brinke, G.; Ikkala, O.; Torkkeli, M.; Serimaa, R. *Macromolecules* **1995**, *28*, 7779.
(22) Ruokolainen, J.; Mäkinen, R.; Torkkeli, M.; Mäkelä, T.; Serimaa, R.; ten Brinke, G.; Ikkala, O. *Science* **1998**, *280*, 557.
(23) Ruokolainen, J.; ten Brinke, G.; Ikkala, O. *Adv. Mater.* **1999**, *11*, 777.
(24) Bondzic, S.; de Wit J.; Polushkin, E.; Schouten, A. J.; ten Brinke, G.; Ruokolainen, J.; Ikkala, O.; Dolbnya, I.; Bras, W. *Macromolecules* **2004**, *37*, 9517.
(25) Kim, S. H.; Misner, M. J.; Xu, T.; Kimura, M.; Russell, T. P. *Adv. Mater.* **2004**, *16*, 226.
(26) Sidorenko, A.; Tokarev, I.; Minko, S.; Stamm, M. *J. Am. Chem. Soc.* **2003**, *125*, 12211.
(27) Keller, A.; Pedemonte, E.; Willmouth, F. M. *Nature (London)* **1970**, *225*, 538; *Kolloid Z. Z. Polym.* **1970**, *238*, 2329.
(28) Hadziioannou, G.; Mathis, A.; Skoulios, A. *Colloid Polym. Sci.* **1979**, *257*, 136. Hadziioannou, G.; Picot, C.; Skoulios, A.; Ionescu, M.-L.; Mathis, A.; Duplessix, R.; Gallot, Y.; Lingelser, J.-P. *Macromolecules* **1982**, *15*, 263.
(29) Koppi, K.; Tirrell, M.; Bates, F. S.; Almdal, K.; Colby, R. H. *J. Phys. II* **1992**, *2*, 1941.
(30) Hamley, I. W.; Pople, J. A.; Fairclough, J. P. A.; Terrill, N. J.; Rayan, A. J.; Booth, C.; Yu, G. E.; Diat, O.; Almdal, K.; Vigild, M.; Mortensen, K. *J. Chem. Phys.* **1998**, *108*, 6929.
(31) Fredrickson, G. H.; Bates, F. S. *Annu. Rev. Mater. Sci.* **1996**, *26*, 501.
(32) Chen, Z.-R.; Kornfield, J. A.; Smith, S. D.; Grothaus, J. T.; Satkowski, M. M. *Science* **1997**, *277*, 1248.
(33) Tepe, T.; Schultz, M. F.; Zhao, J.; Tirrell, M.; Bates, F. S. *Macromolecules* **1995**, *28*, 3008.
(34) Mäkinen, R.; Ruokolainen, J.; Ikkala, O.; De Moel, K.; ten Brinke, G.; De Odorico, W.; Stamm, M. *Macromolecules* **2000**, *33*, 3441.
(35) De Moel, K.; Mäkinen, R.; Stamm, M.; Ikkala, O.; ten Brinke, G. *Macromolecules* **2001**, *34*, 2892.
(36) Bang, J.; Lodge, T. P. *J. Phys. Chem. B* **2003**, *107*, 1207.
(37) Polushkin, E.; Alberda van Ekenstein, G. O. R.; Dolbnya, I.; Bras, W.; Ikkala, O.; ten Brinke, G. *Macromolecules* **2003**, *36*, 1421.
(38) Polushkin, E.; Alberda van Ekenstein, G.; Ikkala, O.; ten Brinke, G. *Rheol. Acta* **2004**, *43*, 364.
(39) Bras, W. *J. Macromol. Sci., Phys.* **1998**, B 37, 557.
(40) Homan, E.; Konijnenburg, M.; Ferrero, C.; Ghosh, R. E.; Dolbnya, I. P.; Bras, W. *J. Appl. Crystallogr.* **2001**, *34*, 519.
(41) Hajduk, D. A.; Takenouchi, H.; Hillmyer, M. A.; Bates, F. S.; Vilild, M. E.; Almdal, K. *Macromolecules* **1997**, *30*, 3788.
(42) Hajduk, D. A.; Ho, R. M.; Hillmyer, M. A.; Bates, F. S.; Almdal, K. *J. Phys. Chem. B* **1998**, *102*, 1356.
(43) Vasilevskaya, V. V.; Gusev, L. A.; Khokhlov, A. R.; Ikkala, O.; ten Brinke, G. *Macromolecules* **2001**, *34*, 5019.
(44) Macosco, C. W. *Rheology Principles, Measurements, and Applications;* VCH Publishers: New York, 1994; p 209.
(45) Spontak, R. J.; Smith, S. D.; Ashraf, A. *Macromolecules* **1993**, *26*, 956.
(46) Hajduk, D. A.; Gruner, S. M.; Rangarajan, P.; Register, R. A.; Fetters, L. J.; Honeker, C.; Albalak, R. J.; Thomas, E. L. *Macromolecules* **1994**, *27*, 490.
(47) Polushkin, E.; Bondzic, S.; Bras, W.; Ikkala, O., ten Brinke, G., to be published.

MA048314K